JOURNAL OF GEOPHYSICAL RESEARCH, VOL. 102, NO. A8, PAGES 17,325-17,333, AUGUST 1, 1997

# Modeling of microburst electron precipitation using pitch angle diffusion theory

S. Datta, R. M. Skoug, M. P. McCarthy, and G. K. Parks

Geophysics Program, University of Washington, Seattle

**Abstract.** Microburst electron precipitation is characterized by short bursty (duration ~0.2-0.3 s) quasiperiodic precipitation of electrons in the dayside auroral zone. Pitch angle diffusion of electrons due to the interaction with whistler waves has been suggested previously as a possible mechanism for scattering electrons into the loss cone to cause microburst precipitation. In this paper we investigate the viability of the above mechanism through modeling. We assume the scattering to occur near the equatorial plane and solve the pitch angle diffusion equation numerically to find the time-dependent form of the electron distribution function $F$, which results from a given time-dependent diffusion coefficient $D$. Different aspects of our results (burst size, pitch angle dependence, risetime, burst width) are compared with observations from a recent rocket experiment on microburst launched from Poker Flat, Alaska. The comparison shows very good agreement, further supporting the idea that the pitch angle diffusion process is the driving mechanism for microbursts.

## Introduction

Microburst, a major form of electron precipitation on the dayside auroral zone (0600-1800 LT), was discovered in the early 1960s [*Anderson and Milton*, 1964]; yet we have very little knowledge about its origin. Microbursts are characterized by short bursty precipitation of electrons (duration ~0.2-0.3 s), often occurring in multiples in a quasiperiodic manner. The well-defined structure and periodicity of microbursts make this phenomenon especially interesting and suggest that a fundamental magnetospheric plasma process is involved in microburst generation. Most of the present state of knowledge on microbursts comes from balloon-borne X ray experiments [*Anderson et al.*, 1966; *Trefall et al.*, 1966; *Parks*, 1967], although primary electron observations have also been reported in a few cases: by *O'Brien et al.* [1964] from Injun 3 satellite data and by *Lampton* [1967] from a rocket experiment. A review article on microbursts is presented by *Parks* [1978].

That a wave-particle interaction may be involved in the generation of microburst was first suggested from a satellite observation by *Oliven and Gurnett* [1968], where microburst occurred only during periods of VLF chorus activity. Other evidence comes from *Rosenberg et al.* [1981], who reported a correlation between microburst precipitation and VLF chorus at conjugate points. *Chang and Inan* [1983] demonstrated through modeling that the cyclotron resonance interaction of electrons with whistlers (right-hand circularly polarized waves) may cause short-scale microburst-like precipitation. This idea was further developed by *Rosenberg et al.* [1990] in association with data from a balloon experiment from Antarctica, where they considered the scattering of electrons due to a wave traveling from the southern to the northern ionosphere along a geomagnetic field line.

The work being presented here is an effort to probe the microburst mechanism through modeling, assisted by the observation of microbursts from a recent sounding rocket experiment designed for this purpose. The rocket instrumentation included two magnetic spectrometers oriented at 0° and 90° to the geomagnetic field measuring electrons in the energy range of 1-25 keV, a set of five solid-state telescopes (SST) oriented at 0°, 22°, 45°, 67°, and 90° detecting 20-300 keV, and an orthogonal pair of loop antennas detecting 0.5-8 kHz VLF waves. The details of the instrumentation and rocket launch conditions are given by *Datta* [1995] and *Skoug* [1995].

The analysis of microburst electron and VLF wave data obtained by the rocket experiment supports the idea that the microburst mechanism involves a wave-particle interaction [*Datta et al.*, 1996; *Skoug et al.*, 1996]. Our observations indicate that the microburst activity was confined to the electron energy range of ~20-120 keV within the interval of ~1-300 keV measured by the experiment. The energy spectrum of microburst flux can be approximated by an exponential form $f = f_0\ E\ e^{-E/E_0}$ (demonstrated with an example in Figure 1, reproduced from *Datta et al.* [1996])



Paper number 97JA00942.
0148-0227/97/97JA-00942$09.00

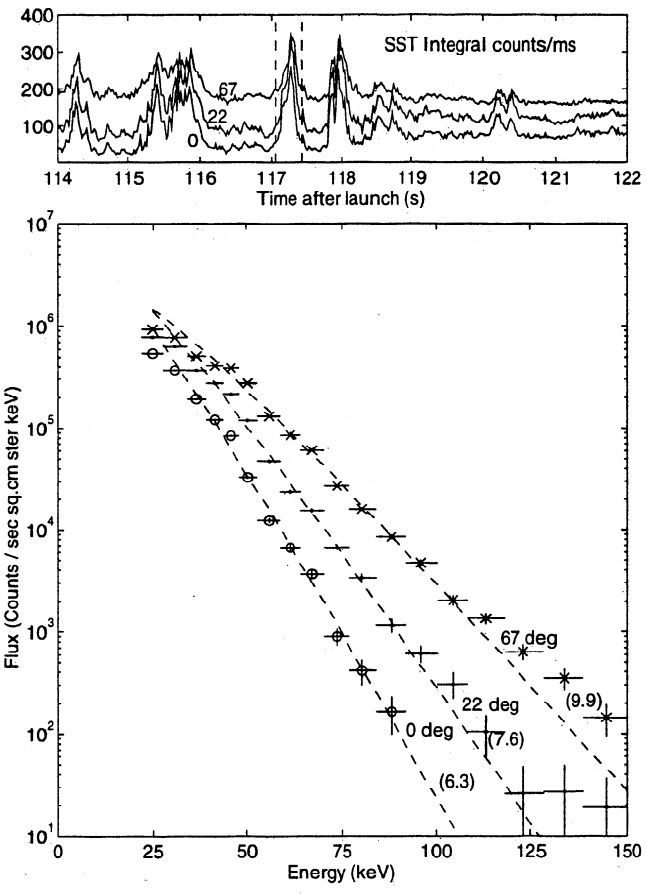


**Figure 1.** (bottom) The electron energy spectra of the microburst at 117.2 s from the 0°, 22°, and 67° solid-state telescopes (SSTs), showing the increase of $E_0$ (in parentheses) with the increase in pitch angle. (top) The corresponding integral count rates (20-300 keV) are plotted.

with an $e$ folding energy of ~6-10 keV along the magnetic field direction. The spectrum becomes progressively harder as the pitch angle increases. For example, the $e$ folding energy at 67° is ~9-11 keV. This behavior can be explained by a steady state model of the pitch angle diffusion process [*Datta et al.*, 1996].

Figure 2 (top) shows 10 s of the rocket electron data, which include several microbursts. The electron flux in the energy range ~20-120 keV from the five SSTs sampling electrons at different pitch angles is shown as a function of time. An important feature to note is that at the peak of the burst, the flux at all pitch angles tends to be equal, indicating that the distribution becomes nearly isotropic. This behavior is different at quieter times in-between the bursts when the flux in the 0° SST goes almost to zero while that at larger pitch angles remains at progressively higher levels. For example, at the peak of the burst ($t$=117.3 s) the ratio of the fluxes from the 0° and 67° SSTs reaches a value of $\sim$ 0.75, whereas before and after the burst ($t$=117.0 and 117.6 s) that ratio is only $\sim$ 0.20.

To show that this behavior is consistent with that expected from a pitch angle diffusion process, consider the analytical form of the steady state electron distribution derived by *Kennel and Petschek* [1966]. Figure 2 (bottom) shows a set of such curves for three different values of the diffusion coefficient $D$ within the equatorial loss cone, which is $\approx$3° at the $L$ shell of 5.9 near the rocket apogee. The vertical lines represent the range of pitch angles sampled by the SSTs at 250 km altitude assuming a dipole field and conservation of the first invariant. Since higher values of $D$ correspond to more electrons diffusing into the loss cone resulting in a higher rate of precipitation, we deduce from Figure 2 that a relative change in the count rate at the rocket altitude when $D$ changes from high to low will be much more pronounced at smaller pitch angles (0° SST) than at larger pitch angles (67° SST), which is what we observe. In the data the flux at 90° is smaller than that at 67° because of the fact that about half of the field of view of the 90° SST does not see downcoming electrons but rather sees reflected electrons, which are much fewer in number at the rocket altitude. This also explains the strong spin modulation ($T_{\rm spin} \approx 1.3$ s) seen by the 90° detector, caused by slight misalignment (~3°) of the rocket spin axis with the geomagnetic field.

*Datta et al.* [1996] did not address the time-varying aspects of the pitch angle diffusion, the importance of which cannot be overemphasized since microbursts are essentially a time-dependent phenomenon. An analytical treatment of this problem involving a time-dependent diffusion coefficient $D(t)$ is extremely difficult. Thus we shall instead investigate this problem in the realm of numerical modeling. The use of a numerical approach will not only give us the capability of treating the time dependence but will also provide us with the flexibility of modeling. For example, we have the freedom of choosing the time profile of the diffusion coefficient. This permits us to model and study the effects of varying $D(t)$ on the risetimes and widths of microburst precipitation.

## Description of the Model

We consider a population of electrons interacting with whistler mode waves near the equatorial region and calculate the corresponding detector responses that we expect at different pitch angles at the rocket location $L \approx 5.8$. The geomagnetic field is considered to be dipolar. The diffusion coefficient $D(t)$ is taken to be independent of pitch angle $\alpha$. We use the distribution function $F$, which represents the density of electrons at different points in phase space. For the discussion of pitch angle diffusion, $F$ in velocity space can be represented as $F(t, v, \alpha)$. Also, we consider electrons within a narrow band of energy so that the distribution function can be written as $F(t, \alpha)$.

Pitch angle diffusion of electrons, caused by interaction with whistler waves, results in the change of the pitch angle $\alpha$ of the electrons without an appreciable change in energy [*Brice*, 1964]. As a result, $F(\alpha)$ also changes. In order to find the resultant temporal varia-

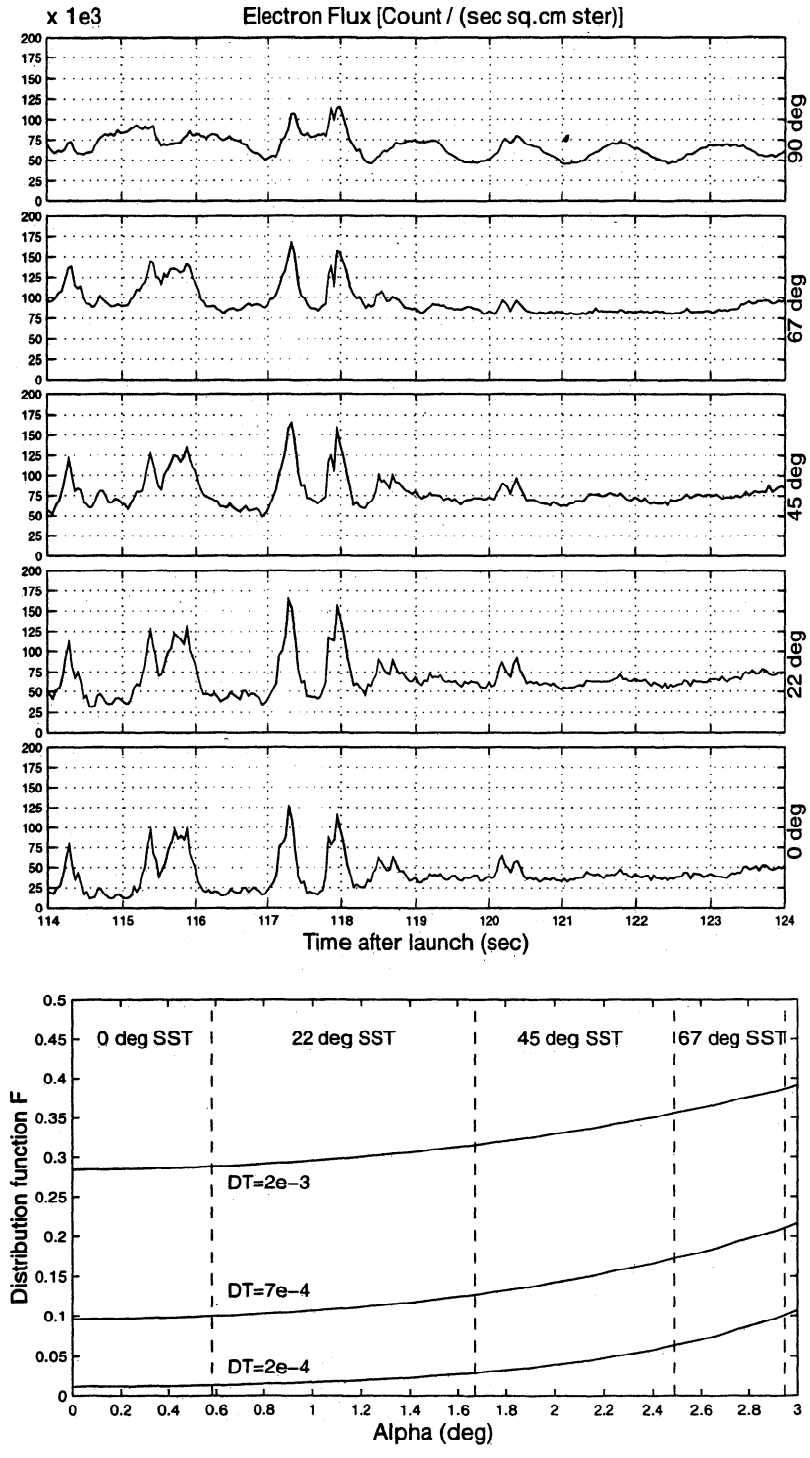


**Figure 2.** (top) Ten seconds of data showing the integral count rates from all five SSTs, with two microbursts at 117.3 and 117.9 s. The features of these data match what one would expect if the pitch angle diffusion process is active, for which case (bottom) the calculated steady state distribution functions $F(\alpha)$ are plotted.

tion of $F(\alpha)$, we numerically solve the time-dependent pitch angle diffusion equation

$$\frac{\partial F}{\partial t} = \frac{1}{\sin\alpha}\frac{\partial}{\partial \alpha}\left( D \sin\alpha \frac{\partial F}{\partial \alpha} \right) \qquad (1)$$

The coefficient of diffusion is defined as $D = \langle(\delta\alpha)^2\rangle/\delta t$, which implies that in time $\delta t$, the electrons diffuse in $\alpha$ in a Gaussian distribution with a standard deviation $\sigma$ of $\delta\alpha = (D \cdot \delta t)^{1/2}$. $D$ is assumed to be pitch angle independent. We divide the electrons into $n$ bins of equal width in pitch angle $\alpha$ ranging from 0° to 90°. We begin with a given initial distribution at $t$=0, described in the next section. The finite difference form of (1) can be written as

$$F_i(t+\Delta t) = F_i(t) + \frac{D\,\Delta t}{\sin\alpha_i\,\Delta_\alpha}\left[\sin\left(\alpha_i+\frac{\Delta_\alpha}{2}\right)\left(\frac{F_{i+1}(t)-F_i(t)}{\Delta_\alpha}\right) - \sin\left(\alpha_i-\frac{\Delta_\alpha}{2}\right)\left(\frac{F_i(t)-F_{i-1}(t)}{\Delta_\alpha}\right)\right] \quad (2)$$

where $F_i$ ($i$ =1 to $n$) are real numbers representing the phase space density in the $i$th bin in $\alpha$. Interpreting physically, the first term within the brackets in (2) represents the total flux of particles from smaller pitch angles, and the second term is that from larger pitch angles. Therefore the finite difference form given above describes the transport of particles in a single time step. This procedure is iterated over many such time steps.

The stability condition for the diffusion equation (see *Forsythe and Wasow* [1960] on parabolic equations) is given by $\lambda = D\Delta t/(\Delta\alpha)^2 \leq \frac{1}{2}$. In our calculation we use $\lambda = 0.15$, ensuring stability as well as good numerical accuracy.

The numerical solution has been carried out in the simplest form (the Euler method), which proved to be sufficient for our purpose since the time durations we looked at typically required only a few hundred time steps and the solution to the diffusion equation using a more sophisticated algorithm (e.g., the Runge-Kutta method) would differ by only <1%. (We are primarily interested in the qualitative behavior.) The numerical code has been tested against the known result of the "very high diffusion" case where the distribution is isotropic in pitch angle. In our algorithm we normalize the total population at every time step, which is equivalent to replenishing the electrons that are lost in the loss cone with a source of electrons of the same pitch angle distribution. Different schemes can also be used, for example, regenerating uniformly over $\alpha$ (equivalent to an isotropic source) or regenerating at $\alpha = 90°$ (the flat pitch source as used by *Kennel and Petschek* [1966]). However, these variations would not change the results significantly since the diffusion lifetime of electrons ($\gtrsim$1000 s), i.e., the time taken for an electron to randomly walk from $\alpha = 90°$ to 0°, is much larger than the microburst timescale. Also, the same reasoning indicates that the $\alpha$ dependence of $D$ (which was taken to be proportional to $\cos\alpha$ by *Kennel and Petschek* [1966] and independent of $\alpha$ in our calculation) will have very little effect on the general precipitation characteristics as long as $D$ is fairly constant in and near the loss cone, which is a reasonable assumption since the resonance condition only involves $v_\parallel$ and all the electrons have the same $v_\parallel$ in a small loss cone as in our case.

## An Example: Evolution from a Very Low Diffusion State

In order to demonstrate how the simulation works, as well as to point out some features of model dependence, we simulate the evolution of the distribution function $F$ when the value of the diffusion coefficient $D$ switches between two levels $D_{\text{low}}$ and $D_{\text{high}}$ in a square wave manner.

If the diffusion activity is preceded by a quiet period, it is reasonable to assume that at $t$=0 the form of the distribution function $F$ is the limiting case $D \to 0$ of the more generalized solution to the pitch angle diffusion equation for electrons injected at a 90° pitch angle [*Kennel and Petschek*, 1966],

$$F = \frac{S}{D^*}\left\{h(\alpha_0) + \ln\left(\frac{\sin\alpha}{\sin\alpha_0}\right)\right\} \quad (3)$$

where $h(\alpha_0)$ is the value of $F$ at the loss cone boundary and $S$ and $D^*$ are constants associated with the intensity of the electron source and pitch angle diffusion, respectively. The loss cone is virtually empty at this point since for very low diffusion the particles diffuse into the loss cone at a much slower rate than they are lost from within the loss cone. Therefore, using $h(\alpha_0) \approx 0$ for $D \to 0$, $F$ can be approximated as

$$F = 0 \quad \alpha < \alpha_0$$
$$F = F_0 \ln\left(\frac{\sin\alpha}{\sin\alpha_0}\right) \quad \alpha > \alpha_0 \quad (4)$$

## Loss Cone Scheme

The evolution of the electron distribution depends both on how the new electrons are injected into the system and how they are lost. Since we are interested in the distribution within the loss cone, the latter factor is of significant importance. *Kennel and Petschek* [1966] assumed that the loss rate in the loss cone is proportional to the value of the distribution function,

$$\frac{\partial F}{\partial t} = \frac{F}{T_E} \quad (5)$$

which implies that if the diffusion process stops suddenly, the population within the loss cone will fall exponentially with a timescale of $T_E$ (escape time of an electron from the interaction region). Although this leads to a nice analytical solution, the validity of this assumption is questionable since the electrons that are in the loss cone at some instant are expected to be completely lost (precipitated in the atmosphere) within an average time period of $T_B$, where $T_B$ is the quarter bounce period (definition of loss cone). In our simulation a different scheme for the loss cone will be used. We shall assume that if a population $P$ of electrons comes into the loss cone at some instant, it will decrease in number at a uniform rate $P/T_B$ until all the electrons are lost in time $T_B$.

Figure 3 shows a sample run. Figure 3a shows the rocket data (integral counts from the 0° and 67° SSTs) showing two microbursts. Figure 3b shows a chosen temporal profile of the diffusion coefficient $D(t)$ given as input. The simulation predicts the variation of the count rates in the 0° and 67° SSTs as a function of time. These traces, calculated using the new and the old loss cone schemes, are shown in Figures 3c and 3d

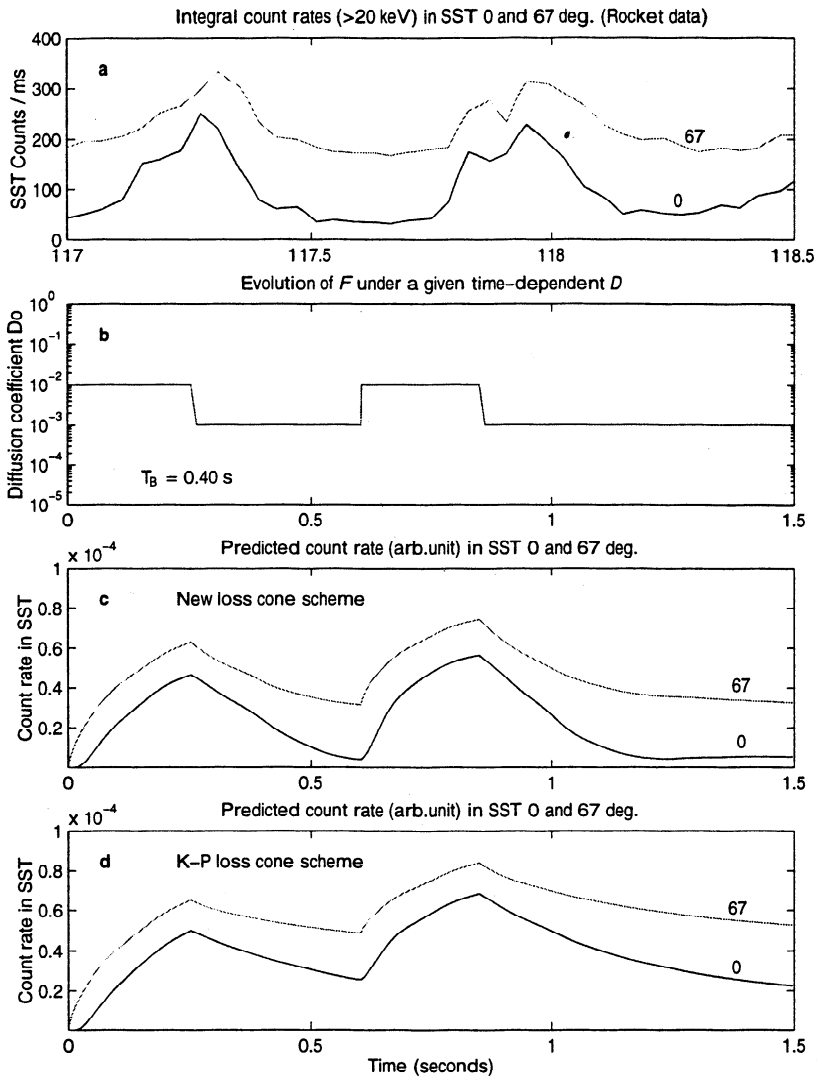


**Figure 3.** (a) A section of our rocket data (from 0° and 67° SST detectors), including two microbursts. (b) A sample run of our simulation, showing a given time profile of $D(t)$. (c) The predicted variation of count rate in those two detectors, using the new loss cone scheme. (d) The scheme used by *Kennel and Petschek* [1966]. Comparing the simulation results with observations, we find that the new scheme describes the data more accurately.

respectively. Comparing the two, we find that the new scheme fits the data more accurately.

In the above discussion we ignored the effect of backscattering of electrons from the atmosphere, which causes a fraction of the primary electrons to be scattered back with some energy degradation. A study by *Davidson* [1986] showed that for a spectrum with $E_0 \approx 10$ keV, as in our case, the number of backscattered (slightly degraded primary) electrons falls below 5% of the downcoming population for all energies, which justifies ignoring this effect for the first order calculation. Backscattering also causes the generation of a large number of secondary electrons, which can travel back to the source region and may affect the whistler characteristics to some extent by changing the total electron density. However, since those secondary electrons have significantly lower energies, the population of the energetic electrons, which is our main concern, is unlikely to be affected by this process. Therefore our assumption of complete loss at the first bounce seems reasonable and is supported by the comparison of Figures 3c and 3d.

## Variation of the Relative Count Rates at Different Pitch Angles Due to the Variation of the Microburst Intensity

Microbursts vary in intensity. While it can be anticipated intuitively that a larger value of the diffusion coefficient $D$ will cause a larger amplitude in electron counts by diffusing electrons at a higher rate into the loss cone, we need to verify whether the relative count rates at different pitch angles predicted by our model agree with the observations. As an example, Figures 4a and 4d show the SST 0° and 67° count rates (standardized after geometric factor and dead time correction) for microbursts of two different amplitudes. For the smaller microburst (Figure 4a) a large difference exists

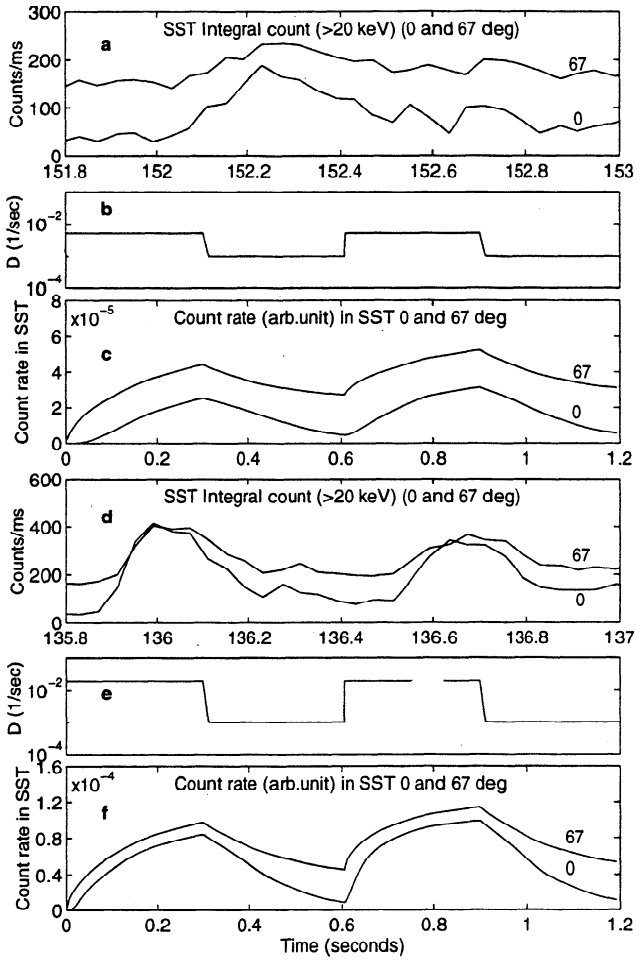


**Figure 4.** Figures 4a-4c show the electron data, diffusion coefficient used in the simulation, and the predicted count rate for a relatively small amplitude microburst. Figures 4d-4f show the same for a larger microburst.

in the count rate between the 0° and 67° SSTs, even at the peak of the burst. For the larger burst (Figure 4d), the count rates in those two detectors become almost equal at the peak, although during the quiet time, the 0° count rate is substantially lower than that at 67°.

In order to study these two situations we choose a square wave profile for $D(t)$. A base value of $D = D_{\text{low}} = 1 \times 10^{-3}/\text{s}$ is used in both cases, but the high-level value is chosen to be relatively lower ($D_{\text{high}} = 5 \times 10^{-3}/\text{s}$) in the first case, and higher ($D_{\text{high}} = 2 \times 10^{-2}/\text{s}$) in the second case. The results of this simulation are shown in Figure 4. Temporal profiles of $D(t)$ in the two cases mentioned above are plotted in Figures 4b and 4e. The corresponding count rates at the 0° and 67° detectors are shown in Figures 4c and 4f. The estimated count rates show qualitative agreement with the main features of our data (Figures 4a and 4d): a higher count rate for a larger value of the diffusion coefficient, dependence of the relative count rates of the 0° and 67° SSTs on the magnitude of the burst, and the relative difference in count rates during quiet times.

The results presented above are not sensitive to the the choice of $D_{\text{low}}$ since the distribution $F$ barely changes during a low diffusion period. The values of $D_{\text{high}}$ were somewhat arbitrarily chosen at this point, and their validity was verified by a test particle simulation in which a number of individual electrons interact with a whistler wave. For the typical wave intensities observed in the frequency band 1200-2100 Hz (which resonate with 20-120 keV microburst electrons for $N_e = 1 \times 10^6/\text{m}^3$ equatorial electron density) the simulation yielded a diffusion intensity of $\sim 3 \times 10^{-3}/\text{s}$. Note that this estimation should be taken as the lower limit of the actual value of $D$ since the waves probably have lost some intensity because of spreading and absorption before reaching the rocket. Therefore our choices of the value of $D$ are in reasonable agreement with the observational data.

### Risetime of Electron Count Rate

We next investigate the dependence of the risetimes of the count rate in the particle data on the timescales of the escape times of electrons from the interaction region. If we assume that the length of the interaction region is the same for electrons of all energies, then the escape time is proportional to the quarter bounce period $T_B$. Moreover, if we assume the interaction region is well extended along the field line, then the time of escape of electrons can be taken as approximately equal to $T_B$.

As before, we take the time profile of $D(t)$ as a step function. Mathematically, $D$ can be represented by a step function,

$$\begin{aligned} D &\ll D_0 \quad t < t_0 \\ D &= D_0 \quad t > t_0. \end{aligned} \tag{6}$$

We again start from the very low diffusion state given by (4). The results are shown in Figure 5. In Figure 5a the simulated count rate at the 0° detector is plotted as a function of time for different values of the quarter bounce period $T_B$, showing that the risetime is approximately proportional to $T_B$. Electron data from the corresponding energy channels of the 0° SST are plotted in Figure 5b. The same trend is observed in both the data and the simulation, i.e., a systematic decrease in the risetime with the increase of electron energy, suggesting that our model is on the right track.

This calculation was done for $L$=5.8. It should also be noted that since we took the time of escape of electron from the interaction region $T_E$ to be equal to the quarter bounce period $T_B$ and the model shows good agreement with the data, indications are that the interaction region is not confined locally at the equatorial plane, but rather it spans a substantial length on both sides of equator along the $B$ field line.

### Pulse Width Dependence

One of the distinctive characteristics of microbursts is their typical burst width (the duration of the burst)

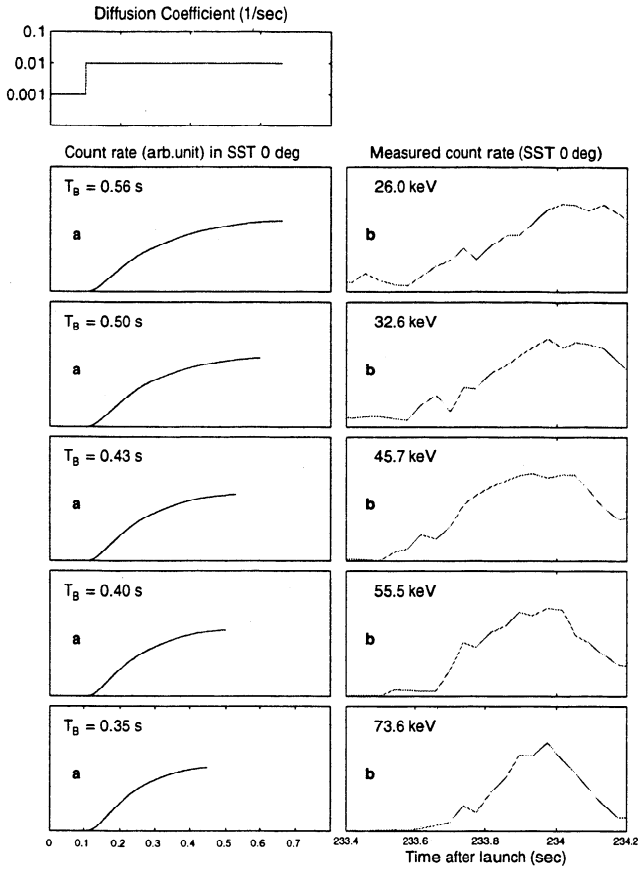


**Figure 5.** For a step function profile of $D(t)$, (a) the estimated risetime of the electron count rate at the 0° detector is approximately proportional to the quarter bounce period $T_B$. This is in agreement with observation at right. (b) Electron from the corresponding energy channels of the 0° SST.

of ~0.2-0.3 s. Next we investigate how this burst width in the particle data depends on the width (duration) of a pulse in the diffusion coefficient $D(t)$. We continue to use the square wave pulse in $D(t)$, switching between the two levels $D_{\text{low}} = 5 \times 10^{-4}$ /s and $D_{\text{high}} = 2 \times 10^{-2}$ /s. The electron escape time $T_E$ is taken as 0.4 s, approximately equal to the average value of $T_B$ of microburst electrons. The results for a field-aligned detector are shown in Figure 6. Here we consider the variation of the full width at half maximum (FWHM) of the electron precipitation, which is the width of a peak measured between two points on the two sides of the peak where the intensities are half of the peak maximum. The FWHM of the electron precipitation stays fairly constant as long as the width $W_D$ of the square wave pulse in $D(t)$ is small, and as $W_D$ increases, the FWHM slowly approaches the value $W_D$, as expected. The constancy of $W_D$ for short pulses in $D(t)$ also implies that there is a minimum width for bursts produced by changes in $D(t)$.

These results are important since they provide some clue about the reason behind the microburst characteristic width. We see from Figure 6, for instance, that when $W_D$ changes from 0.1 to 0.3 s, the FWHM of the resultant electron burst changes by only about 40%. This slow functional dependence of FWHM on $W_D$ tells us that as long as $W_D$ is less than or equal to the quarter bounce period $T_B$, it will cause a pulse in the electron count rate within a fairly narrow range of widths. Therefore, if the magnetospheric conditions are such that the wave enhancements occur in short bursts ($\lesssim T_B$), that will result in the occurrence of particle precipitation with a temporal width of ~0.2-0.3 s, or microburst-like structures.

### Effect of Different Temporal Profiles of $D(t)$

So far we have used a square pulse in the diffusion coefficient $D(t)$ while varying the other factors. This is an idealization only, and in reality we do not expect the enhancement of the diffusion coefficient to occur in a square pulse. Moreover, the temporal structure of microbursts can be widely different in overall shape and microstructures, as observed in our rocket data.

To observe how the expected electron count rate depends on the variation of the diffusion coefficient $D(t)$, we ran our program with several different temporal profiles of $D(t)$, shown in Figure 7. For example, we assumed the rise of the diffusion pulse to be linear, exponential, or abrupt and also used similar variations of the fall time. Such variations in $D(t)$ do result in different shapes of the electron count rate, though the characteristic width of the electron pulse is found to be conserved. This suggests that variations in the microburst structure may be a consequence of the variation of the diffusion coefficient profile.

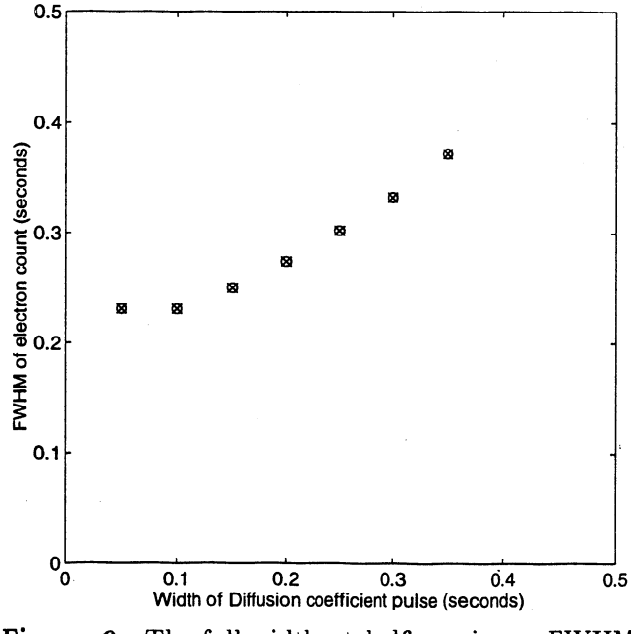


**Figure 6.** The full width at half maximum FWHM of the electron count rate as a function of the corresponding pulse width of $D(t)$, showing that the electron FWHM is insensitive to that of $D(t)$ to some extent.

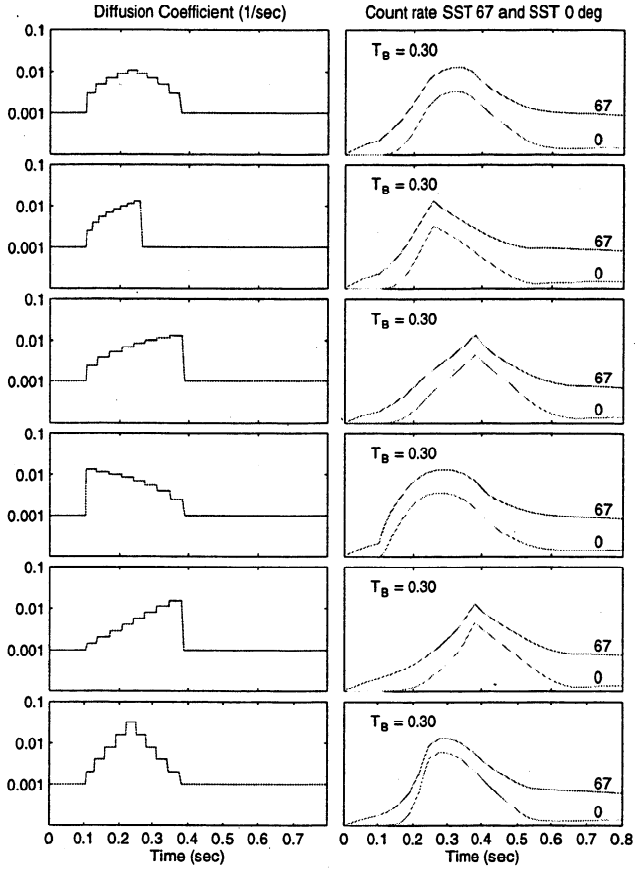


**Figure 7.** (left) Different time profiles in $D(t)$ and (right) the resultant count rates in the 0° and 67° detectors.

## Summary and Discussion

The results from our model of the evolution of the electron distribution function indicate that the pitch angle diffusion process near the equatorial plane is responsible for microburst electron precipitation. The model correctly predicts several features of microbursts, which include the relative count rates of precipitated electrons observed by the rocket experiment at different pitch angles and for different diffusion intensities (Figure 4), as well as the general shape of microbursts (Figure 3) and their rapid fall time (~0.2 s). We estimated the magnitude of the diffusion coefficient at the microburst peak to vary between $5\times10^{-3}$/s and $2\times10^{-2}$/s. The microburst risetime as a function of electron energy is also estimated (Figure 5) and compares with the rocket data quite favorably. Most importantly, the simulation establishes the apparent insensitivity of the microburst pulse width to that of the diffusion activity when the diffusion pulse width is small, thus giving a possible explanation of the characteristic width of microbursts (Figure 6). The actual shape of individual microburst electron pulses is observed to vary within a large range. This is explained to be due to different temporal profiles of the diffusion coefficient.

One should bear in mind that the validity of the results from these simulations only holds strictly under a set of assumptions and approximations. For example, the diffusion coefficient $D$ has been assumed to be independent of $\alpha$. The $\alpha$ dependence could be implemented to investigate this effect. $D$ may also be nonuniform along the field line, and the use of a time-averaged $D = \int D_{\text{local}}(1/Tv)ds$ would be meaningful. However, because of the lack of knowledge of the local value $D_{\text{local}}$, we use an effective $D$ that is constant over the interaction region and zero outside. Also, the energy diffusion (change in energy of electrons), which is inherently associated with the pitch angle diffusion, has not been taken into account since it is quite small in the situation we are describing. As an example, near the equatorial plane at $L = 5.8$ and for $N_e = 1\times10^6/\text{m}^3$ the value of $\Delta E/\Delta\alpha$ for a 30 keV electron is only ~ 0.3 keV/deg near the loss cone, which justifies the idea that energy diffusion effects can be ignored.

The constancy of the physical conditions over the whole interaction region is inherently assumed, even when the region is extended. The rationale behind that assumption is that near the equatorial plane both $B$ and $\partial B/\partial s$ are at a minimum (as are the pitch angle $\alpha$ and number density $N_e$) and the spatial variations are very low over an extended region, which allows us to assume the constancy of the parameters over the region of interaction. This approximation keeps the calculation simple while still letting us see the qualitative aspects. A more complete study will also include the spatial dependence of the physical parameters such as the number density and pitch angle, a detailed study of the energy dependence to construct the energy spectrum, and an investigation of the $L$ shell dependence of the diffusion.

One other important consideration is the dispersion effect, which is the relative delay of arrival of electrons in different energy channels. In our data we saw less dispersion than would be expected for an equatorial source, assuming that electrons of all energies are scattered into the loss cone simultaneously and at the same location. Probably neither of these two conditions are strictly valid in our case since the whistler wave may move and interact with electrons of different energies at different points along the field line. We have done a preliminary modeling study of a group of whistler waves moving along a field line while precipitating electrons whose energy depends on the location. Our simulation does show the expected reduction of the dispersion effect. This result is not conclusive, and a more detailed analysis is being done. However, the results presented here are not affected by this consideration since our model does not require any assumption of the relative time of scattering of different energies.

So far we have assumed a priori the presence of diffusion activity (or equivalently, wave enhancement), but the cause of that and the source of energy required for this wave growth have not been addressed here. The possibility of self-induced wave growth in a wave-

particle system (i.e., the gain of wave energy at the cost of the energy of electrons moving toward the loss cone) is being considered as an explanation. The available energy for wave growth is likely to depend on various physical conditions, for example, the density of precipitating electrons, the whistler characteristics, and the electron energy. This work is being undertaken and will be presented in another paper.

**Acknowledgments.** The authors thank S. Werden for his contribution at various stages of the rocket experiment, R. Winglee for useful discussions on numerical modeling, and T. Chinowsky and J. Chin for their work on the rocket electronics. The authors also thank D. Moltedo and his team at the NASA Wallops Flight Facility, Virginia, for the integration and launch of the rocket. This work was supported by NASA grant NAGW-2009.

The editor thanks R. B. Horne and another referee for their assistance in evaluating this paper.

## References

Anderson, K. A., and D. W. Milton, Balloon observations of X rays in the auroral zone, *J. Geophys. Res.*, *69*, 4457, 1964.

Anderson, K. A., L. M. Chase, H. S. Hudson, M. Lampton, D. W. Milton, and G. K. Parks, Balloon and rocket observations of auroral-zone microbursts, *J. Geophys. Res.*, *71*, 4617, 1966.

Brice, N., Fundamentals of very low frequency emission generation mechanisms, *J. Geophys. Res.*, *69*, 4515, 1964.

Chang, H. C., and U. S. Inan, A theoretical model study of observed correlations between whistler mode waves and energetic electron precipitation events in the magnetosphere, *J. Geophys. Res.*, *88*, 10053, 1983.

Datta, S., The analysis and modeling of microburst electron precipitation using pitch-angle diffusion theory, Ph.D. thesis, Univ. of Wash., Seattle, 1995.

Datta, S., R. M. Skoug, M. P. McCarthy, and G. K. Parks, Analysis and modeling of microburst precipitation, *Geophys. Res. Lett.*, *23*, 1729, 1996.

Davidson, G. T., Pitch angle diffusion in morningside aurorae, 1, The role of the loss cone in the formation of impulsive bursts of precipitation, *J. Geophys. Res.*, *91*, 4413, 1986.

Forsythe, G. E., and W. R. Wasow, *Finite-Difference Methods for Partial Differential Equations*, John Wiley, New York, 1960.

Kennel, C. F., and H. E. Petschek, Limit on stably trapped particle fluxes, *J. Geophys. Res.*, *71*, 1, 1966.

Lampton, M., Daytime observations of energetic auroral-zone electrons, *J. Geophys. Res.*, *72*, 5817, 1967.

O'Brien, B. J., C. D. Laughlin, and D. A. Gurnett, High-latitude geophysical studies with satellite Injun 3, 1, Description of the satellite, *J. Geophys. Res.*, *69*, 1, 1964.

Oliven, M. N., and D. A. Gurnett, Microburst phenomena, 3, An association between microbursts and VLF chorus, *J. Geophys. Res.*, *73*, 2355, 1968.

Parks, G. K., Spatial characteristics of auroral zone X ray microbursts, *J. Geophys. Res.*, *72*, 215, 1967.

Parks, G. K., Microburst precipitation phenomena, *J. Geomagn. Geoelectr.*, *30*, 327, 1978.

Rosenberg, T. J., J. C. Siren, D. L. Matthews, K. Marthinsen, J. A. Holtet, A. Egeland, D. L. Carpenter, and R. A. Helliwell, Conjugacy of electron microbursts and VLF chorus, *J. Geophys. Res.*, *86*, 5819, 1981.

Rosenberg, T. J., R. Wei, D. L. Detrick, and U. S. Inan, Observations and modeling of wave-induced microburst electron precipitation, *J. Geophys. Res.*, *95*, 6467, 1990.

Skoug, R. M., The origin of narrow band cyclotron wave emissions called chorus, Ph.D. thesis, Univ. of Wash., Seattle, 1995.

Skoug, R. M., S. Datta, M. P. McCarthy, and G. K. Parks, A cyclotron resonance model of VLF chorus emissions detected during electron microburst precipitation, *J. Geophys. Res.*, *101*, 21481, 1996.

Trefall, H. J., W. E. Bjordal, S. L. Ullaland, and J. Stadsma, On the extension of auroral-zone X ray microbursts, *J. Atmos. Terr. Phys.*, *28*, 225, 1966.

---

S. Datta, R. M. Skoug, M. P. McCarthy, and G. K. Parks, University of Washington, Geophysics Program, Box 351650, Seattle, WA 98195-1650.

(Received November 25, 1996; revised March 21, 1997; accepted March 24, 1997.)